PHYSICAL REVIEW D **88,** 034014 (2013)

$K \to \pi\pi$ hadronic matrix elements of left-right current-current operators

Stefano Bertolini*
INFN, Sezione di Trieste, SISSA, via Bonomea 265, 34136 Trieste, Italy

Alessio Maiezza†
Università dell'Aquila, Via Vetoio, Coppito, 67100 L'Aquila, Italy

Fabrizio Nesti‡
Gran Sasso Science Institute, Viale Crispi 7, 67100 L'Aquila, Italy
(Received 29 May 2013; published 8 August 2013)

Effective $\Delta S = 1$ four-fermion operators involving left- and right-handed currents are relevant in left-right gauge extensions of the Standard Model and scalar extension of the Yukawa sector. They induce $K \to \pi\pi$ decays which are strictly constrained by experimental data, typically resulting in strong bounds on the new physics scales or parameters. We evaluate the $K \to \pi\pi$ hadronic matrix elements of such operators within the phenomenological framework of the chiral quark model. The results are consistent with the estimates used in a previous work on TeV scale left-right symmetry, thus confirming the conclusions obtained there.

DOI: 10.1103/PhysRevD.88.034014 PACS numbers: 13.25.Es, 12.39.Ki, 12.39.Fe, 12.60.−i

I. INTRODUCTION

The enduring successes of the Standard Model (SM), in particular in the quark flavor sector, naturally provide stringent tests and constraints on new physics (NP) theoretical modeling. An historical and relevant role in testing NP models is played by the CP-violating $\Delta S = 1, 2$ processes in kaon physics. It is in fact a common feature of NP scenarios the presence of additional flavor-changing (FC) interactions that induce new effective operators at the electroweak scale. The presence of such operators often leads to sharp constraints on the scales and the couplings of the extended theory.

A paradigmatic example is the left-right (LR) extension of the SM [1–5], which in its minimal version provides a complete theory of neutrino masses [6], and directly connects possible new accelerator (LHC) physics to lower energy phenomena like neutrinoless double-beta decay and lepton flavor violation [7] (for a recent review see e.g. Ref. [8]). In the quark sector, flavor changing operators lead to a lower bound on the right-handed gauge boson scale slightly above the TeV region [9], within the reach of LHC searches. LR symmetric models generate a new set of FC operators (a complete set for $\Delta S = 1$ can be found in [10]) some of which turn out to be crucially relevant for phenomenology.

Characteristic of the LR setup are the following current-current operators:

$$Q_1^{LR} = (\bar{s}_\alpha u_\beta)_L(\bar{u}_\beta d_\alpha)_R, \qquad Q_1^{RL} = (\bar{s}_\alpha u_\beta)_R(\bar{u}_\beta d_\alpha)_L,$$
$$Q_2^{LR} = (\bar{s}u)_L(\bar{u}d)_R, \qquad Q_2^{RL} = (\bar{s}u)_R(\bar{u}d)_L, \tag{1}$$

where the subscripts L, R stand for $\gamma_\mu(1 \pm \gamma_5)$ and α, β are color indices, understood in Q_2. In the LR models these operators are generated at tree level by gauge boson exchange and thus have a prominent role in setting constraints on the model parameters [9,11]. They are as well generated in other popular NP extensions of the SM, as for instance supersymmetry, with FC processes driven by squark mediation, or extended Higgs models with FC interactions (for a systematic discussion on flavor physics beyond the SM see Ref. [12]).

As mentioned above the operators (1) play a role in $\Delta S = 1$ processes and they are particularly relevant for the study, within NP models, of direct CP violation in $K \to \pi\pi$ decay, namely for the calculation of the ε' parameter. In order to match the experimental precision, the $K \to \pi\pi$ matrix elements of the effective operators are needed beyond the simple and naive factorization. First principle approaches to nonperturbative QCD (of which lattice is the foremost) have not yet provided an accurate and reliable answer. In this work we address this issue by offering a (phenomenological) calculation of such matrix elements in the framework of the chiral quark model (χQM) [13–20].

To this aim, we construct and determine, via the integration of the constituent quark fields of the χQM, the $\Delta S = 1$ chiral Lagrangian relevant to $Q_{1,2}^{LR,RL}$ at $O(p^2)$ in the momentum expansion. The chiral coefficients are generally determined within the model in terms of three nonperturbative parameters, namely the constituent quark mass M, the quark condensate $\langle\bar{q}q\rangle$ and the gluon condensate $\langle\frac{\alpha_s}{\pi}GG\rangle$. Their values and model ranges were phenomenologically determined in Ref. [21] via the fit of the $\Delta I = 1/2$ selection rule in $K \to \pi\pi$ decays, which eventually lead to the successful prediction of ε'/ε [22]. Such a phenomenological and self-contained determination of

*stefano.bertolini@sissa.it
†alessio.maiezza@aquila.infn.it
‡nesti@aquila.infn.it

the model parameters represents in our opinion the strength of the approach and it is at the root of the robustness of the results.

Consistency with the needed order in momentum expansion requires the inclusion of the chiral loops contributions to the $K \to \pi\pi$ amplitudes, that we compute. Eventually, we provide the $O(p^2)$ matrix elements via the B parameters, which gauge the departure from the vacuum saturation approximation (VSA). The B parameters are given at the intrinsic χQM scale of about 0.8 GeV, as well as at 2 GeV, for direct comparison with forthcoming lattice calculations.

II. THE $\Delta S = 1$ CHIRAL LAGRANGIAN (MAKING OF)

The quark $\Delta S = 1$ effective Lagrangian is written as a combination of local quark operators

$$\mathcal{L}_{\Delta S=1} = \Sigma_i C_i(\mu) Q_i(\mu), \tag{2}$$

where Q_i are effective four-quark operators as in Eq. (1) and C_i are their short-distance Wilson coefficients, evaluated at a scale μ. By extending the SM to include right-handed interactions, the sum in Eq. (2) spans a complete set of 28 operators [10], which exhibit all chiral combinations of L, R currents.

Contact with the physical mesonic transitions is made once the relevant hadronic matrix elements of the effective quark operators are computed. Since the relevant scale for kaon physics falls in the strong interacting regime of QCD, the problem cannot be addressed with perturbative (coupling expansion) methods. In the present work we address this issue by means of a phenomenological approach based on the χQM.

The χQM takes advantage of the QCD chiral symmetry while introducing an effective quark-meson interaction. This provides a bridge between the perturbative QCD and chiral Lagrangian regimes. The model can be seen as the mean-field approximation of an extended Nambu-Jona-Lasinio model that mimics QCD at intermediate energies [23,24]. After integrating out the constituent quark fields, the meson octet interactions are determined in terms of three nonperturbative parameters: the constituent quark mass, the quark condensate and the gluon condensate. The model is renormalizable in the large-N_c limit [25] and it is successful in reproducing the $O(p^4)$ low energy constants of the Gasser-Leutwyler Lagrangian as well as a number of observables, albeit one must be aware of its limitations [26,27].

In the 1990s a thorough investigation of the $\Delta S = 1$ and $\Delta S = 2$ chiral Lagrangians within the framework of the χQM has been carried out [21,22,28,29]. The project led to a successful prediction of the direct CP violation in $K \to \pi\pi$ decays $(\varepsilon'/\varepsilon)$ shortly before its experimental determination. The approach was based on the self-consistent determination of the nonperturbative parameters of the χQM via the fit of the CP conserving $\Delta I = 1/2$ selection rule in $K \to \pi\pi$. Such a phenomenological setup was central to reducing the model systematic uncertainties and to providing a robust prediction.

While, ultimately, first principle approaches to nonperturbative QCD (lattice being the foremost; see Ref. [30] for recent developments) must provide the evaluations of hadronic transitions, here we apply the χQM phenomenological approach to the calculation of the $K \to \pi\pi$ matrix elements of the LR current-current operators (1).

A. The chiral quark model

In the χQM a meson-quark interaction term is added to the ordinary QCD Lagrangian:

$$\mathcal{L}_M = -M(\bar{q}_R \Sigma q_L + \bar{q}_L \Sigma^\dagger q_R), \tag{3}$$

where $q = (uds)^t$ and $\Sigma \equiv e^{\frac{2i}{f}\Pi(x)}$, $\Pi(x)$ being the $SU(3)$ meson octet acting on the fundamental representation. The parameter M is identified as the constituent quark mass, as it follows from a chiral quark rotation that absorbs Σ in the constituent quark fields (henceforth referred to as the "rotated" picture):

$$\mathcal{L}_M = -M(\bar{Q}_R Q_L + \bar{Q}_L Q_R), \tag{4}$$

where $q_L = \xi^\dagger Q_L$, $q_R = \xi Q_R$, with $\Sigma = \xi^2$ and $\Sigma^\dagger = (\xi^\dagger)^2$, respectively. In the rotated picture the quark-meson interactions arise from the quarks kinetic term, as

$$\mathcal{L}_{\text{int}} = \bar{Q}(\gamma^\mu V_\mu + \gamma^\mu \gamma_5 A_\mu) Q, \tag{5}$$

the vector and axial fields V_μ and A_μ being defined as

$$\begin{aligned} V_\mu &= \frac{i}{2}(\xi^\dagger \partial_\mu \xi + \xi \partial_\mu \xi^\dagger), \\ A_\mu &= \frac{i}{2}(\xi^\dagger \partial_\mu \xi - \xi \partial_\mu \xi^\dagger). \end{aligned} \tag{6}$$

Analogously, in the rotated description the ordinary quark mass term

$$\mathcal{L}_m = \bar{q}_R \mathcal{M} q_L + \bar{q}_L \mathcal{M}^\dagger q_R, \tag{7}$$

with $\mathcal{M} = \text{diag}\{m_u, m_d, m_s\}$, becomes

$$\mathcal{L}_m = \bar{Q}_R \xi^\dagger \mathcal{M} \xi^\dagger Q_L + \bar{Q}_L \xi \mathcal{M}^\dagger \xi Q_R. \tag{8}$$

B. Bosonic representation of the quark operators

The χQM provides a systematic way of constructing the bosonic representation of the effective $\Delta S = 1$ quark operators in Eq. (2) [28]. By integrating out the constituent quarks, an effective chiral Lagrangian is generated:

$$\mathcal{L}_{\Delta S=1} = \sum_{i,j} G_j(Q_i) O_j^\chi, \tag{9}$$

where O_j^χ are bosonic operators involving the octet meson fields and $G_j(Q_i)$ are the chiral coefficients determined by the matching with the χQM Lagrangian.

We are now set to construct the chiral representation of the $Q_{1,2}^{LR}$ operators. It is sufficient to consider the LR operators, as the RL ones are related to the former by symmetry. Up to the color structure, both $Q_{1,2}^{LR}$ have the form

$$\bar{q}_L \lambda_1^3 \gamma^\mu q_L \bar{q}_R \lambda_2^1 \gamma_\mu q_R \tag{10}$$

that in the rotated picture reads

$$\bar{Q}_L \xi \lambda_1^3 \gamma^\mu \xi^\dagger Q_L \bar{Q}_R \xi^\dagger \lambda_2^1 \gamma_\mu \xi Q_R. \tag{11}$$

The flavor projectors λ_i^j are appropriate matrices such that $\bar{q}\lambda_i^j q = \bar{q}_j q_i$, for $i, j = 1, 2, 3$.

For any such four-quark operator, the effective bosonic operators in the chiral Lagrangian arise by integrating out the quarks Q, while inserting in all possible ways either two A_μ fields of Eq. (6), or $\xi^\dagger \mathcal{M} \xi^\dagger$, $\xi \mathcal{M}^\dagger \xi$ from Eq. (8) in the constituent quark loops. Since V_μ transforms as a gauge field, terms involving the vector field break local chiral invariance and cannot appear in the $O(p^2)$ chiral Lagrangian [17–19]. Both the operators in Eq. (11) and their fierzed forms can be used [28]. By applying this procedure to $Q_{1,2}^{LR}$ we obtain at $O(p^2)$

$$\begin{aligned}\mathcal{L}_{\Delta S=1} = {}& \bar{G}_0(Q_{1,2}^{LR})\,\mathrm{Tr}[\lambda_1^3 \Sigma^\dagger \lambda_2^1 \Sigma] + \bar{G}_m(Q_{1,2}^{LR})\{\mathrm{Tr}[\lambda_2^1 \Sigma \lambda_1^3 \Sigma^\dagger \mathcal{M} \Sigma^\dagger] + \mathrm{Tr}[\lambda_1^3 \Sigma^\dagger \lambda_2^1 \Sigma \mathcal{M}^\dagger \Sigma]\} \\ &+ \bar{G}_{LR}^a(Q_{1,2}^{LR})\,\mathrm{Tr}[\lambda_2^3 D^\mu \Sigma]\,\mathrm{Tr}[\lambda_1^1 D_\mu \Sigma^\dagger] + \bar{G}_{LR}^b(Q_{1,2}^{LR})\,\mathrm{Tr}[\lambda_1^3 \Sigma^\dagger D^\mu \Sigma]\,\mathrm{Tr}[\lambda_2^1 \Sigma D_\mu \Sigma^\dagger] \\ &+ \bar{G}_{LR}^c(Q_{1,2}^{LR})\{\mathrm{Tr}[\lambda_2^3 \Sigma]\,\mathrm{Tr}[\lambda_1^1 D_\mu \Sigma^\dagger D^\mu \Sigma \Sigma^\dagger] + \mathrm{Tr}[\lambda_2^3 D_\mu \Sigma D^\mu \Sigma^\dagger \Sigma]\,\mathrm{Tr}[\lambda_1^1 \Sigma^\dagger]\},\end{aligned} \tag{12}$$

where we used $A_\mu = -\frac{i}{2}\xi(D_\mu \Sigma^\dagger)\xi = \frac{i}{2}\xi^\dagger(D_\mu \Sigma)\xi^\dagger$ and flavor trace rearrangements [28].

The term proportional to $\bar{G}_0$ corresponds to no axial field insertion. The terms $\bar{G}_{LR}^{a,b,c}$ arise from the insertion of two axial fields A_μ, while $\bar{G}_m$ corresponds to the insertion of $\mathcal{L}_m$, Eq. (8) [22]. We use the notation $\bar{G}$ to distinguish them from the analogous SM chiral coefficients G in Ref. [28]. In our calculation we take $m_u = m_d = 0$, so that the relevant contribution to $\bar{G}_m$ is proportional to m_s.

III. CALCULATION OF THE CHIRAL COEFFICIENTS

In the χQM the amplitudes for processes involving external mesons are evaluated through quark loops connected by a given operator insertion, and quark-meson interactions as given for instance by Eq. (3) in the unrotated picture. The contribution to the chiral coefficients G_i of a given quark operator is computed by matching the χQM amplitude for a conveniently chosen mesonic transition with the same amplitude obtained from the expansion of the chiral Lagrangian (12).

At order $O(p^2)$, and for the operators considered, five coefficients $\bar{G}_0$, $\bar{G}_m$, $\bar{G}_{LR}^{a,b,c}$ are present, thus requiring five independent matching equations. We will choose below to calculate the off-shell transitions $K^0 \to \pi^0$ and $K^+ \to \pi^+$, together with the on-shell $K \to \pi^+\pi^-$, $K \to \pi^0\pi^0$ decay amplitudes. Expanding in the quark mass one of the off-shell transitions will then determine $\bar{G}_m$.

For the regularization of the divergent integrals we use dimensional regularization ($d = 4 - 2\epsilon$). The "quadratic" ($\epsilon - 1$ pole) and logarithmic (ϵ pole) divergences serve as a bookkeeping device to identify the "bare" quark condensate and the meson decay constant, namely [23,24]

$$\langle \bar{q}q \rangle^{(0)} = -\frac{N_c M^3}{4\pi^2}\left(\frac{4\pi\tilde{\mu}^2}{M^2}\right)^\epsilon \Gamma(\epsilon - 1), \tag{13}$$

$$f^{(0)} = \frac{N_c M^2}{4\pi^2 f}\left(\frac{4\pi\tilde{\mu}^2}{M^2}\right)^\epsilon \Gamma(\epsilon), \tag{14}$$

where N_c is the number of colors. We replace below these bare parameters with the physical ones $\langle \bar{q}q \rangle$ and f. This automatically includes in the chiral coefficients the factorizable gluon condensate corrections that are needed to recover the numerical consistency of the parameters, in particular of $\langle \bar{q}q \rangle$. It is also worth mentioning that Eqs. (13) and (14) imply a relation between the two bare quantities. This ambiguity, intrinsic to the regularization scheme, becomes numerically irrelevant when all the contributions to the amplitudes at a given order are included. Finally, at the one-loop level in the chiral expansion [and at $O(p^2)$ in the momentum expansion] f will be further identified with the renormalized decay constant f_1, that reproduces the correct pion and kaon decay constants [21].

A. Constituent quark loops

With one insertion of the four-fermion operators, the constituent quark loops appear in two possible patterns, the so-called factorized or the unfactorized form [28], corresponding to two distinct or a single Dirac trace. The amplitude is evaluated considering all the possible ways the desired process is realized by attaching the meson fields to the quark loops. This is best performed in the unrotated picture. As an example the off-shell process $k^+ \to \pi^+$ is represented in Fig. 1. The way color indices are saturated in the quark operator determines which diagrams are leading or subleading in $1/N_c$. For the case of Q_2^{LR}, the first diagram in Fig. 1 is of $O(N_c)^2$ whereas the last two are of $O(N_c)$. The opposite occurs for Q_1^{LR}.

The direct computation in the naive dimensional regularization (NDR) γ_5 scheme of the diagrams in Fig. 1 for the $Q_{1,2}^{LR}$ operators leads to

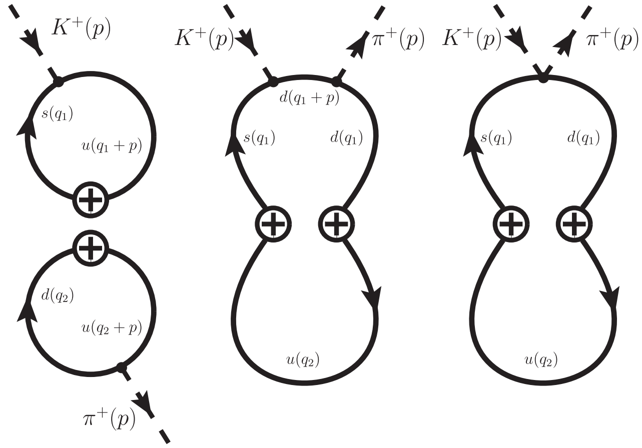

FIG. 1. Diagrams leading to the off-shell $K^+ \to \pi^+$ transition within the χQM, in the unrotated quark picture. The black points represent the meson-quark vertices, while the crossed circles represent the four-quark operator insertion. The loop momenta are q_1 and q_2. The two configurations of constituent quark loops correspond to the product of two distinct Dirac traces or to a single one.

$$\langle \pi^+|Q_1^{LR}|K^+\rangle_{\mathrm{NDR}} = \frac{2i}{3}\left[3\langle \bar{q}q\rangle\left(\frac{\langle \bar{q}q\rangle}{f^2} + m_s\right) - f^2p^2\right] - \frac{6iM^2}{\Lambda_\chi^2}[2f^2p^2 + M(f^2m_s + \langle \bar{q}q\rangle)] \quad (15)$$

and

$$\langle \pi^+|Q_2^{LR}|K^+\rangle_{\mathrm{NDR}} = \frac{2i}{3}\left[\langle \bar{q}q\rangle\left(m_s + \frac{\langle \bar{q}q\rangle}{f^2}\right) - 3f^2p^2\right] - \frac{2iM^2}{\Lambda_\chi^2}[2f^2p^2 + M(f^2m_s + \langle \bar{q}q\rangle)], \quad (16)$$

where $\Lambda_\chi = 2\pi\sqrt{6/N_c}f_\pi \simeq 0.82$ GeV [28] is the natural cutoff of the theory and f_π is the pion decay constant. The two amplitudes exhibit a leading term and a subleading one in the M^2/Λ_χ^2 expansion.

Similar results are found in the 't Hooft–Veltman (HV) γ_5 scheme:

$$\langle \pi^+|Q_1^{LR}|K^+\rangle_{\mathrm{HV}} = \frac{2i}{3}\left[3\langle \bar{q}q\rangle\left(\frac{\langle \bar{q}q\rangle}{f^2} + m_s\right) - f^2p^2\right] - \frac{12iM^2f^2p^2}{\Lambda_\chi^2}, \quad (17)$$

$$\langle \pi^+|Q_2^{LR}|K^+\rangle_{\mathrm{HV}} = \frac{2i}{3}\left[\langle \bar{q}q\rangle\left(m_s + \frac{\langle \bar{q}q\rangle}{f^2}\right) - 3f^2p^2\right] - \frac{4iM^2f^2p^2}{\Lambda_\chi^2}, \quad (18)$$

which differ from Eqs. (15) and (16) only by subleading terms in M^2/Λ_χ^2.

The corresponding expressions for the $K \to \pi^+\pi^-$ and $K \to \pi^0\pi^0$ on-shell processes are also found by direct evaluation of the quark loops in the unrotated picture. These processes involve a fairly large number of diagrams and we do not report here the detailed expressions.

By matching all mesonic amplitudes with the corresponding transitions obtained from the expansion of the chiral Lagrangian (12) we determine the chiral coefficients $\bar{G}_0$, $\bar{G}_m$ and $\bar{G}_{LR}^{a,b,c}$ up to order $O(p^2)$. The results are reported in Table I, in both the NDR and HV γ_5 schemes.

The chiral coefficients depend on the quark condensate $\langle \bar{q}q\rangle$ and on the f parameter. The latter will be eventually identified, after inclusion of the $O(p^2)$ wave function renormalization and of the chiral loop corrections to the leading-order term ($\bar{G}_0$) of the amplitude, with the $O(p^2)$ decay constant parameter f_1 [21].

Some subtleties arise during the calculation. Namely, in the NDR scheme one is not allowed to use Fierz rotations and, as consequence, both the factorized and unfactorized calculations have to be performed. In the HV scheme fierzing is allowed that simplifies the calculation, but one must be aware of the possible presence of "fake" chiral anomalies (see for instance [31]), and convenient subtractions have to be implemented in the chiral Lagrangian [28]. This implies, among else, that $\bar{G}_{LR}^b$ can be computed in both schemes from factorized diagrams, and as a consequence it does not depend on the γ_5 scheme. This holds also for $\bar{G}_{LR}^c$ that turns out to be subleading in M^2/Λ_χ^2. In this case, the vanishing of the leading contribution is immediately seen by considering the bosonization of the fierzed operator.

TABLE I. The contributions of $Q_{1,2}^{LR}$ to the chiral coefficients in Eq. (12) as computed in the χQM, in the HV and NDR renormalization schemes.

	HV	NDR
$\bar{G}_0(Q_1^{LR})$	$-2\langle \bar{q}q\rangle^2$	$-2\langle \bar{q}q\rangle^2\left(1 - \frac{3M^3f^2}{\langle \bar{q}q\rangle\Lambda_\chi^2}\right)$
$\bar{G}_m(Q_1^{LR})$	$-2f^2\langle \bar{q}q\rangle$	$-2f^2\langle \bar{q}q\rangle\left(1 - \frac{3M^2}{\Lambda_\chi^2}\right)$
$\bar{G}_{LR}^a(Q_1^{LR})$	$2\frac{f^2\langle \bar{q}q\rangle}{M}$	$2\frac{f^2\langle \bar{q}q\rangle}{M}\left(1 - \frac{3M^2}{\Lambda_\chi^2}\right)$
$\bar{G}_{LR}^b(Q_1^{LR})$	$-\frac{f^4}{3}$	$-\frac{f^4}{3}$
$\bar{G}_{LR}^c(Q_1^{LR})$	$-\frac{6Mf^2\langle \bar{q}q\rangle}{\Lambda_\chi^2}$	$-\frac{6Mf^2\langle \bar{q}q\rangle}{\Lambda_\chi^2}$
$\bar{G}_0(Q_2^{LR})$	$-\frac{2}{3}\langle \bar{q}q\rangle^2$	$-\frac{2}{3}\langle \bar{q}q\rangle^2\left(1 - \frac{3M^3f^2}{\langle \bar{q}q\rangle\Lambda_\chi^2}\right)$
$\bar{G}_m(Q_2^{LR})$	$-\frac{2}{3}f^2\langle \bar{q}q\rangle$	$-\frac{2}{3}f^2\langle \bar{q}q\rangle\left(1 - \frac{3M^2}{\Lambda_\chi^2}\right)$
$\bar{G}_{LR}^a(Q_2^{LR})$	$\frac{2}{3}\frac{f^2\langle \bar{q}q\rangle}{M}$	$\frac{2}{3}\frac{f^2\langle \bar{q}q\rangle}{M}\left(1 - \frac{3M^2}{\Lambda_\chi^2}\right)$
$\bar{G}_{LR}^b(Q_2^{LR})$	f^4	f^4
$\bar{G}_{LR}^c(Q_2^{LR})$	$-\frac{2Mf^2\langle \bar{q}q\rangle}{\Lambda_\chi^2}$	$-\frac{2Mf^2\langle \bar{q}q\rangle}{\Lambda_\chi^2}$

It is interesting to mention that the results for the chiral coefficients induced by the $8_L \otimes 8_R$ $Q_{1,2}^{LR}$ operators are common to any four-quark LR operator of the form (10), with an arbitrary choice of flavor projectors, which transform in general as $(8+1)_L \otimes (8+1)_R$. This is best understood in the rotated picture, where one can treat the flavor projectors λ_i^j as spurions, that eventually appear in the diverse operators in the chiral Lagrangian (12) without affecting the values of the coefficients. In practice the coefficients are $SU(3)$ invariant, as long as they depend on chirally symmetric parameters. One may in fact verify that the results given in Table I for $Q_{1,2}^{LR}$ coincide with those obtained in Refs. [21,22] for the operators $\Delta Q_{8,7}$ that differ in the flavor structure and transform as $8_L \otimes (8+1)_R$. This result is nontrivial in the unrotated picture as the number and the topology of the diagrams involved in the bosonization and in the computation of the chiral coefficients for the two sets of operators do crucially depend on the flavor indices. In passing, let us also mention that when computing the isospin 2 component of the $K \to \pi\pi$ amplitude the difference between the $Q_{1,2}^{LR}$ and $\Delta Q_{8,7}$ operators vanishes. In the chiral limit this implies a relation among the $Q_{1,2}^{LR}$ and $Q_{8,7}$ contributions to A_2 on which we will comment in the following.

In Table I subleading $1/N_c$ corrections due to the gluon condensate $\langle \frac{\alpha_s}{\pi} GG \rangle$ are neglected. The values of the nonperturbative χQM parameters, namely M, $\langle \bar{q}q \rangle$ (and $\langle GG \rangle$), are phenomenologically determined by the successful fit of the $\Delta I = 1/2$ selection rule in $K \to \pi\pi$, as explained in Ref. [21].

IV. $K^0 \to \pi\pi$ MATRIX ELEMENTS AT $O(p^2)$

A. Chiral loops

In the previous section we have computed the chiral coefficients, induced by the quark operators $Q_{1,2}^{LR}$, at $O(p^2)$ which, in the case at hand, is next to leading order in the momentum expansion. In order to consistently compute the $K \to \pi\pi$ amplitudes in the chiral expansion, we must include the corrections due to the relevant chiral loops. Again, it is enough to focus on the $Q_{1,2}^{LR}$ operators, since the matrix elements of the RL ones have the opposite sign due to parity.

Using the standard decomposition of the $K \to \pi\pi$ amplitudes in isospin zero and two, $A_0 = (2A_{\pm} + A_{00})/\sqrt{6}$, $A_2 = (A_{\pm} - A_{00})/\sqrt{3})$, it is also useful to parametrize them as

$$A_{0,2} = A_{0,2}^{\chi_0} + A_{0,2}^{\chi_1}, \tag{19}$$

where the superscripts $\chi_{0,1}$ refers to the tree and one-loop chiral contributions, respectively.

The tree-level isospin amplitudes for both $Q_{1,2}^{LR}$ read

$$A_0^{\chi_0} = \frac{1}{\sqrt{3} f^3}[4\bar{G}_0 Z_\pi \sqrt{Z_K} + 4\bar{G}_m m_s + \bar{G}_{LR}^a (3m_K^2 + m_\pi^2) + 2\bar{G}_{LR}^b (m_K^2 - m_\pi^2) + \bar{G}_{LR}^c (2m_K^2 - 9m_\pi^2)], \tag{20}$$

$$A_2^{\chi_0} = -\frac{1}{f^3}\sqrt{\frac{2}{3}}[\bar{G}_0 Z_\pi \sqrt{Z_K} + \bar{G}_m m_s + \bar{G}_{LR}^a m_\pi^2 + \bar{G}_{LR}^b (m_K^2 - m_\pi^2) - \bar{G}_{LR}^c m_K^2], \tag{21}$$

where Z_π and Z_K are the one-loop wave function renormalizations within the χQM [21]:

$$Z_\pi = 1 - 2\frac{m_\pi^2}{\Lambda_\chi^2}, \qquad Z_K = 1 - 2\frac{m_K^2}{\Lambda_\chi^2} + 6\frac{M m_s}{\Lambda_\chi^2} \tag{22}$$

(neglecting terms proportional to the up and down quark masses).

Some care must be taken in computing the tree-level component of the amplitudes proportional to $\bar{G}_0$, since the related chiral operator [the first in Eq. (12)] allows for a nonvanishing $K \to 0$ transition that must be rotated away, in agreement with the Feinberg-Kabir-Weinberg theorem [32].

At the one-loop level in chiral perturbation theory, vertex and wave function renormalizations due to chiral loops appear, which are displayed in Figs. 2 and 3, respectively. We evaluate the chiral loops in dimensional regularization

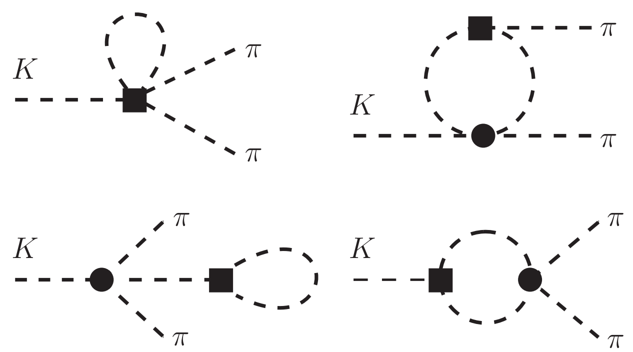

FIG. 2. Chiral loop vertex renormalization of $K \to \pi\pi$. The internal states are all the allowed $SU(3)$ octet mesons. The square box represents the weak vertex, while the circle represents the insertion of a strong vertex.

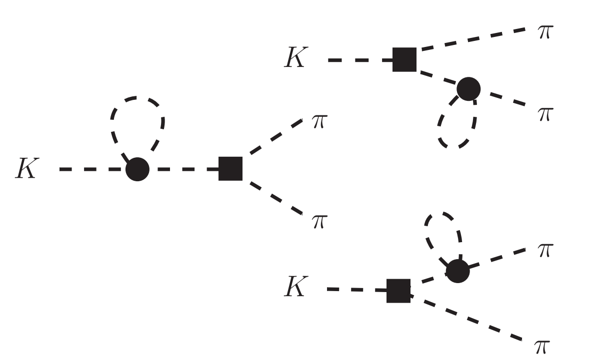

FIG. 3. Chiral loop wave function renormalization for the $K \to \pi\pi$ transitions. The square box and the circle represent the weak and the strong vertex, respectively. All allowed $SU(3)$ octet mesons are exchanged in the loop.

TABLE II. Values of the physical parameters and phenomenological ranges of the nonperturbative χQM parameters used in the numerical analysis.

f_π	0.092 GeV
f_K	0.113 GeV
m_π	0.137 GeV
m_K	0.498 GeV
m_η	0.547 GeV
Λ_χ	0.82 GeV
f_1	$0.087^{+0.012}_{-0.014}$ GeV
M	$0.200^{+0.005}_{-0.003}$ GeV
$\langle\bar{q}q\rangle$	$-(0.240^{+0.030}_{-0.010}\text{ GeV})^3$

and subtract the divergences according to the $\overline{\rm MS}$, consistently with the χQM determination of the chiral coefficients.

At order $O(p^2)$ only the chiral loop corrections to the $\bar{G}_0$ term need to be included. The resulting analytical expressions for the amplitudes are complicated polynomial and logarithmic functions of the meson masses. We find it useful to report the following seminumerical forms of the isospin amplitudes:

$$A_0^{\chi_1} = \frac{4}{\sqrt{3}}\frac{\bar{G}_0 f_\pi^2}{f^5}[1.36 + 0.46i + 0.46\ln\mu^2], \tag{23}$$

$$A_2^{\chi_1} = \sqrt{\frac{2}{3}}\frac{\bar{G}_0 f_\pi^2}{f^5}[0.20 + 0.20i + 0.051\ln\mu^2], \tag{24}$$

where μ is in units of GeV, and we have explicitly factored the tree-level amplitudes in front. The numerical coefficients correspond to the values of the meson parameters given in Table II. The absorptive part of the amplitudes stems from the last diagram in Fig. 2, as it follows from the Cutkosky cuts. We stress though that in order to obtain the absorptive part at a given order in the perturbative expansion the amplitude must be evaluated at the next order.

These expressions allow us to appreciate the impact of the chiral loops on the full amplitudes. While they are small in the isospin-two amplitude, the isospin-zero projection receives a sizable chiral loop renormalization, that is responsible for most of its deviation from the VSA, as we shall discuss next.

It is worth noting that the chiral corrections to the A_2 amplitude, Eq. (24), coincide numerically with those computed for the operators $\Delta Q_{8,7}$ in Ref. [22], as mentioned at the end of the previous section. This is due to the fact that the $\Delta Q_{8,7}$ and $Q_{1,2}^{LR}$ share the same $\Delta I = 3/2$ component [33].

B. The B parameters

A convenient way to show the results is to normalize the $K \to \pi\pi$ matrix elements to their VSA values. By denoting $\langle Q\rangle_{0,2} = \langle\pi\pi, I = 0,2|Q|K\rangle$, where the subscripts refer to the isospin components, the B parameters are defined as

$$B_{0,2} \equiv \frac{\mathrm{Re}\langle Q\rangle_{0,2}^{\rm model}}{\langle Q\rangle_{0,2}^{\rm VSA}}. \tag{25}$$

The reference VSA values for the Q_1^{LR} operator can be written as [11]

$$\langle Q_1^{LR}\rangle_0^{\rm VSA} = \frac{\sqrt{2}(X + 9Y + 3Z)}{3\sqrt{3}}, \tag{26}$$

$$\langle Q_1^{LR}\rangle_2^{\rm VSA} = \frac{1}{3}\sqrt{\frac{1}{3}}(X - 6Z), \tag{27}$$

and similarly for Q_2^{LR}

$$\langle Q_2^{LR}\rangle_0^{\rm VSA} = \frac{\sqrt{2}(3X + 3Y + Z)}{3\sqrt{3}}, \tag{28}$$

$$\langle Q_2^{LR}\rangle_2^{\rm VSA} = \frac{1}{3}\sqrt{\frac{1}{3}}(3X - 2Z), \tag{29}$$

where $X \equiv i\sqrt{2}f_\pi(m_K^2 - m_\pi^2)$, $Y \equiv i\sqrt{2}f_K A^2$, $Z \equiv i\sqrt{2}f_\pi A^2$, respectively, and $A \equiv m_K^2/(m_s + m_d)$.

By taking the scale μ at the chiral perturbation theory cutoff $\Lambda_\chi \simeq 0.82$ GeV (where the values for the nonperturbative parameters M and $\langle\bar{q}q\rangle$ in Table II were obtained in [21]) and spanning over the model parameter space, we obtain the values for the different $B_{0,2}(Q_{1,2}^{LR})$. In Fig. 4 the contour levels of B_0 and B_2 as a function of the relevant χQM parameters are displayed. Both HV and NDR schemes results are shown. As one can see, the γ_5-scheme dependence is quite limited since it appears at $O(M^2/\Lambda_\chi^2)$.

The numerical summary of $B_{0,2}$ for the two LR operators is reported in Table III (the same values hold for the RL related operators). Their uncertainties are evaluated by considering the variation of the relevant parameters, namely M, $\langle\bar{q}q\rangle$, f_1 and m_s. The parameters f_1 and $\langle\bar{q}q\rangle$ have a correlated variation range, displayed as the shaded ellipses in Fig. 4. The correlation stems from the dependence on f_1 and $\langle\bar{q}q\rangle$ on the next to leading order low energy constant L_5 in the strong chiral Lagrangian as computed in the χQM (see Appendix B in Ref. [21]), namely

$$L_5 = -\frac{f_1^4}{8M\langle\bar{q}q\rangle}\left(1 - 6\frac{M^2}{\Lambda_\chi^2}\right), \tag{30}$$

by taking into account the present uncertainty on the knowledge of L_5 (about 10%). This correlated variation drives most of the final uncertainty in B_0, B_2, the effect of the constituent quark mass M and of its correlation being numerically irrelevant. We have consistently (and conservatively) used for the strange quark mass its partial conservation of axial current (PCAC) value $m_s(\mu) = -f_\pi^2 m_K^2/\langle\bar{q}q\rangle(\mu)$, which for the range of the quark

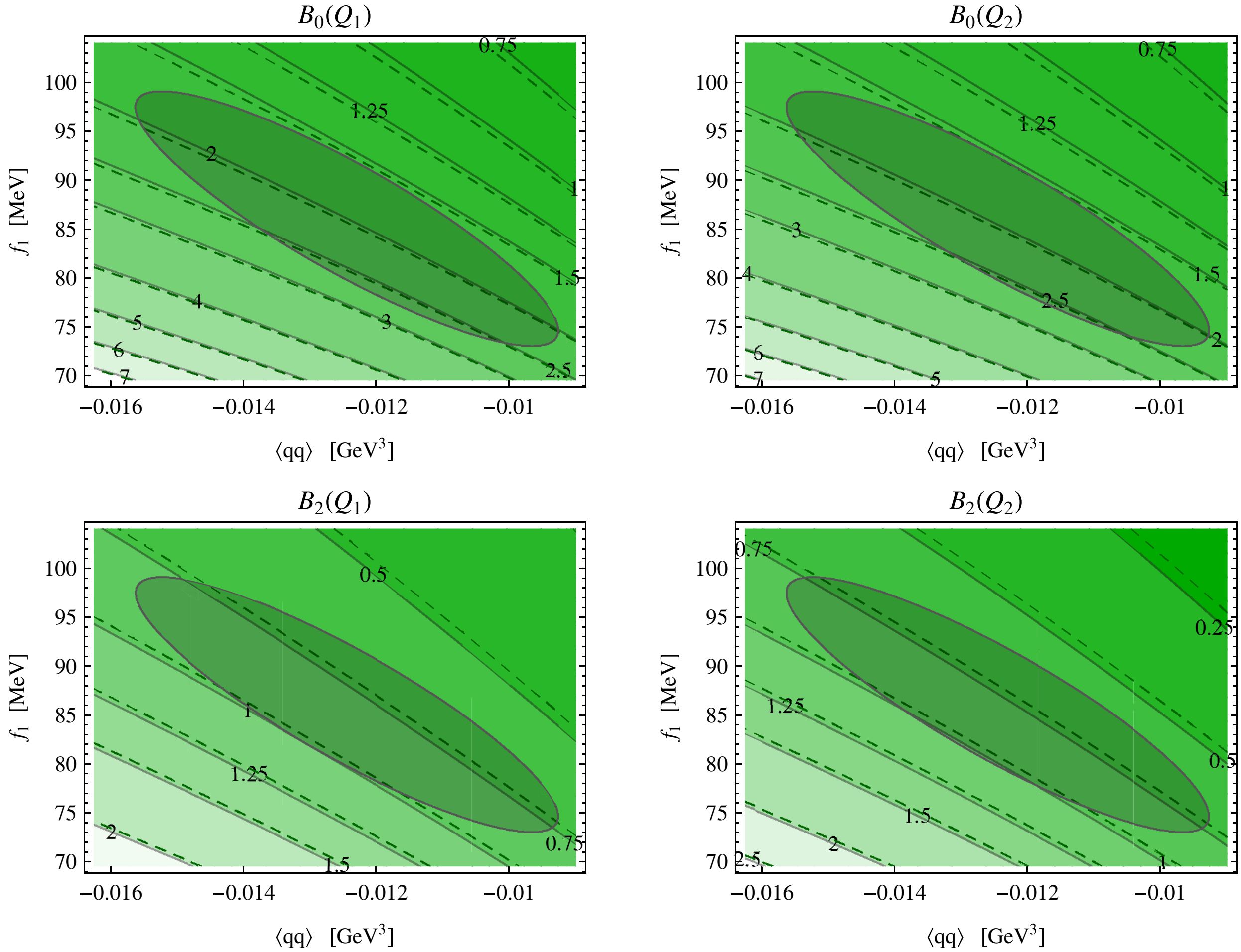

FIG. 4 (color online). Contour levels of B_0 and B_2 for $Q_1^{LR,RL}$ (left) and $Q_2^{LR,RL}$ (right panels) in the HV and NDR renormalization schemes (continuous and dashed contours, respectively). The ellipse marks the correlated range of the parameters $\langle\bar{q}q\rangle$ and f_1 in the phenomenological fit of the χQM, as discussed in the text.

condensate given in Table II leads to $m_s(\Lambda_\chi) = 152^{+20}_{-45}$ MeV. This is well consistent, albeit with a larger range, with $m_s(2\ \text{GeV}) = 95 \pm 5$ MeV from lattice determinations [34].

The B parameters for the LR current-current operators $Q_{1,2}^{LR}$ turn out to have a size comparable to that of the standard electroweak penguins $Q_{7,8}$ [35]. For the isospin-two component of the amplitudes one expects, on the basis of the symmetry arguments discussed earlier, the parameters $B_2(Q_{1,2}^{LR})$ to be the same as the corresponding $B_2(Q_{8,7})$. The numerical difference is due to the $O(p^4)$ corrections included in Refs. [21,22] and here neglected.

For future reference we also give in Table IV the values of B_0, B_2 at the renormalization scale $\mu = 2$ GeV, calculated by taking into account the anomalous dimension matrix of the $Q_{1,2}^{LR}$ operators [36] as well as the running of $\langle\bar{q}q\rangle$ and m_s (related by PCAC). As one sees, within the uncertainties, the values of B_0 and B_2 can be considered scale independent between Λ_χ and 2 GeV, in agreement with the leading role of the $O(p^0)$ coefficient $\bar{G}_0$ and its dependence on $\langle\bar{q}q\rangle^2$, analogous to the VSA.

TABLE III. Values of B_0 and B_2 at $\mu = 0.82$ GeV for $\langle\pi\pi|Q_{1,2}^{LR,RL}|K\rangle$, in the NDR and HV γ_5 schemes.

	NDR	HV
$B_0(Q_1^{LR,RL})$	$2.00^{+0.87}_{-0.39}$	$2.04^{+0.85}_{-0.40}$
$B_0(Q_2^{LR,RL})$	$1.95^{+0.82}_{-0.37}$	$1.99^{+0.80}_{-0.38}$
$B_2(Q_1^{LR,RL})$	$0.64^{+0.11}_{-0.17}$	$0.62^{+0.11}_{-0.17}$
$B_2(Q_2^{LR,RL})$	$0.59^{+0.14}_{-0.18}$	$0.57^{+0.13}_{-0.18}$

TABLE IV. The same as Table III at $\mu = 2$ GeV.

	NDR	HV
$B_0(Q_1^{LR,RL})$	$1.84^{+0.85}_{-0.36}$	$1.87^{+0.84}_{-0.37}$
$B_0(Q_2^{LR,RL})$	$1.82^{+0.82}_{-0.35}$	$1.84^{+0.81}_{-0.36}$
$B_2(Q_1^{LR,RL})$	$0.55^{+0.09}_{-0.15}$	$0.54^{+0.09}_{-0.15}$
$B_2(Q_2^{LR,RL})$	$0.52^{+0.10}_{-0.15}$	$0.51^{+0.10}_{-0.15}$

V. CONCLUSIONS

In this work we considered the calculation of hadronic matrix elements of the $\Delta S = 1$ left-right four-quark operators $Q_{1,2}^{LR}$ which are present in popular extension of the SM. Because of their possible tree-level origin, they are potentially the source of large contributions of new physics to kaon hadronic decays, thus giving rise to stringent constraints on the new physics scales and/or couplings. A paradigmatic example is the LR symmetric model, where the above operators are generated at a large scale by $W_L - W_R$ mixing. The possibility of a TeV size right-handed scale, together with the absence of loop suppression in the Wilson coefficients, may be the source of sizable contributions of LR current-current operators to direct CP violation in the kaon sector. The $Q_{1,2}^{LR,RL}$ operators are present in minimal extensions of the SM Yukawa sector and in supersymmetry extensions as well.

Among the complete set of $\Delta S = 1$ four-quark operators, these were the only one for which an evaluation of the relevant $\langle \pi\pi | Q_{1,2}^{LR} | K \rangle$ matrix elements was missing. We addressed the calculation of these hadronic matrix elements in the context of the chiral quark model. To this aim, the complete $O(p^2)$ $\Delta S = 1$ effective chiral Lagrangian was constructed. This allowed us to perform a complete evaluation of the $K \to \pi\pi$ matrix elements at $O(p^2)$, which includes the one-loop chiral contributions. The computation was performed in both NDR and HV γ_5 renormalization schemes. The $K \to \pi\pi$ amplitudes for $Q_{1,2}^{LR}$ were found to be similar to those of the standard penguin operators $Q_{7,8}$, respectively (which are partially related to the LR current-current ones by symmetry arguments). We compared our results, obtained at the chiral breaking scale, with those of the simple factorization (VSA), showing deviations within 50%. For a convenient comparison with forthcoming (and hopefully ultimate) lattice results, the values of the matrix elements are also shown at the scale of 2 GeV.

ACKNOWLEDGMENTS

S. B. acknowledges partial support by the Italian MIUR Grant No. 2010YJ2NYW_001 and by the EU Marie Curie ITN UNILHC Grant No. PITN-GA-2009-237920. A. M. acknowledges SISSA for hospitality during the conclusion of this work.

[1] J. C. Pati and A. Salam, Phys. Rev. D **10**, 275 (1974); **11**, 703(E) (1975).
[2] R. N. Mohapatra and J. C. Pati, Phys. Rev. D **11**, 566 (1975).
[3] R. N. Mohapatra and J. C. Pati, Phys. Rev. D **11**, 2558 (1975).
[4] G. Senjanović and R. N. Mohapatra, Phys. Rev. D **12**, 1502 (1975).
[5] G. Senjanović, Nucl. Phys. **B153**, 334 (1979).
[6] M. Nemevšek, G. Senjanović, and V. Tello, Phys. Rev. Lett. **110**, 151802 (2013).
[7] V. Tello, M. Nemevšek, F. Nesti, G. Senjanović, and F. Vissani, Phys. Rev. Lett. **106**, 151801 (2011).
[8] G. Senjanović, Riv. Nuovo Cimento Soc. Ital. Fis. **34**, 1 (2011).
[9] A. Maiezza, M. Nemevšek, F. Nesti, and G. Senjanović, Phys. Rev. D **82**, 055022 (2010).
[10] S. Bertolini, J. O. Eeg, A. Maiezza, and F. Nesti, Phys. Rev. D **86**, 095013 (2012).
[11] G. Ecker and W. Grimus, Nucl. Phys. **B258**, 328 (1985).
[12] A. Buras, Acta Phys. Pol. B **41**, 2487 (2010).
[13] K. Nishijima, Nuovo Cimento **11**, 698 (1959).
[14] F. Gursey, Nuovo Cimento **16**, 230 (1960).
[15] F. Gursey, Ann. Phys. (Paris) **12**, 91 (1961).
[16] J. A. Cronin, Phys. Rev. **161**, 1483 (1967).
[17] S. Weinberg, Physica (Amsterdam) **96A**, 327 (1979).
[18] A. Manohar and H. Georgi, Nucl. Phys. **B234**, 189 (1984).
[19] A. Manohar and G. W. Moore, Nucl. Phys. **B243**, 55 (1984).
[20] D. Espriu, E. de Rafael, and J. Taron, Nucl. Phys. **B345**, 22 (1990); **B355**, 278(E) (1991).
[21] S. Bertolini, J. O. Eeg, M. Fabbrichesi, and E. I. Lashin, Nucl. Phys. **B514**, 63 (1998).
[22] S. Bertolini, J. O. Eeg, M. Fabbrichesi, and E. I. Lashin, Nucl. Phys. **B514**, 93 (1998).
[23] J. Bijnens, C. Bruno, and E. de Rafael, Nucl. Phys. **B390**, 501 (1993).
[24] J. Bijnens, Phys. Rep. **265**, 370 (1996).
[25] S. Weinberg, Phys. Rev. Lett. **105**, 261601 (2010).
[26] E. de Rafael, Phys. Lett. B **703**, 60 (2011).
[27] D. Greynat and E. de Rafael, J. High Energy Phys. 07 (2012) 020.
[28] V. Antonelli, S. Bertolini, J. O. Eeg, M. Fabbrichesi, and E. I. Lashin, Nucl. Phys. **B469**, 143 (1996).
[29] V. Antonelli, S. Bertolini, M. Fabbrichesi, and E. I. Lashin, Nucl. Phys. **B493**, 281 (1997).
[30] P. A. Boyle *et al.* (RBC and UKQCD Collaborations), Phys. Rev. Lett. **110**, 152001 (2013).
[31] M. S. Chanowitz, M. Furman, and I. Hinchliffe, Nucl. Phys. **B159**, 225 (1979).
[32] G. Feinberg, P. Kabir, and S. Weinberg, Phys. Rev. Lett. **3**, 527 (1959).
[33] P. Chen, H. Ke, and X. Ji, Phys. Lett. B **677**, 157 (2009).
[34] J. Beringer *et al.* (Particle Data Group), Phys. Rev. D **86**, 010001 (2012).
[35] S. Bertolini, M. Fabbrichesi, and J. O. Eeg, Rev. Mod. Phys. **72**, 65 (2000).
[36] P. L. Cho and M. Misiak, Phys. Rev. D **49**, 5894 (1994).